Fusion suppression in mass-asymmetric reactions leading to Ra compound nuclei

R. N. Sagaidak,* G. N. Kniajeva, I. M. Itkis, M. G. Itkis, N. A. Kondratiev, E. M. Kozulin, I. V. Pokrovsky, A. I. Svirikhin, V. M. Voskressensky, and A. V. Yeremin
Flerov Laboratory of Nuclear Reactions, Joint Institute for Nuclear Research, 141980 Dubna, Moscow region, Russia

L. Corradi, A. Gadea, A. Latina, A. M. Stefanini, S. Szilner, M. Trotta, and A. M. Vinodkumar
Istituto Nazionale di Fisica Nucleare, Laboratori Nazionali di Legnaro, I-35020 Legnaro, Padova, Italy

S. Beghini, G. Montagnoli, and F. Scarlassara
Dipartimento di Fisica and INFN-Sezione di Padova, Università di Padova, I-35131 Padova, Italy

D. Ackermann
Gesellschaft für Schwerionenforschung mbH (GSI), D-64291 Darmstadt, Germany
and Johannes Gutenberg-Universität, D-55099 Mainz, Germany

F. Hanappe
Université Libre de Bruxelles, PNTPM, CP229, B-1050 Brussels, Belgium

N. Rowley and L. Stuttgé
IReS, UMR7500, IN2P3-CNRS/Université Louis Pasteur, BP28, F-67037 Strasbourg Cedex 2, France
(Received 20 March 2003; published 21 July 2003)

Near-barrier excitation functions have been measured for evaporation-residue production and fission in the $^{12}C+^{204,206,208}Pb$ and $^{48}Ca+^{168,170}Er$ systems that lead to the compound nuclei $^{216,218,220}Ra^*$. A pronounced suppression of evaporation-residue production is observed for the more symmetric combinations, $^{48}Ca+^{168,170}Er$. We relate this to the significant quasifission components already observed for these systems.

DOI: 10.1103/PhysRevC.68.014603 PACS number(s): 25.70.Gh, 25.70.Jj

Much progress has been achieved in the study of fusion reactions, leading to nonfissile medium-mass compound nuclei [1], through the direct measurements of the resulting evaporation residue (ER) cross sections and their interpretation in terms of potential-barrier distributions. It is clear, however, that a description of heavy-ion fusion with massive partners must go beyond the conventional potential-barrier-passing models applicable to such medium-mass systems. Experiments [2–6] show that for two massive nuclei, the compound nucleus formation is strongly reduced at incident energies around the nominal fusion barrier [7] due to the quasifission (QF) process. This is clearly manifested in the comparison of the ER cross sections for reactions leading to the same compound nucleus but having different mass asymmetries in the entrance channel [8,9]. Rather unexpectedly, QF is even manifested in fairly asymmetric combinations with ^{19}F and ^{30}Si projectiles leading to the $^{216}Ra^*$ compound nucleus (CN) [10].

Of course, QF forms the part of the barrier-passing (capture) cross section, and we may write $\sigma_{bp}=\sigma_{QF}+\sigma_{CN}$. That is the system may evolve to form a fully equilibrated CN (fuse) or may retain a dinuclear character leading to QF. The fused CN may then cool by evaporation of particles to yield long-lived ERs, or may itself undergo fission: (CN fission): $\sigma_{CN}=\sigma_{ER}+\sigma_{fis}$. We thus ultimately have two fission components, one which passed through the CN phase (fis) and the other which did not (QF). Of course, the detection of ERs is an unambiguous signature of fusion since they can only come from the CN configuration and not through the QF process.

The decay of a CN is subject to shell effects in the decay chains that lead to the final residues and, for massive nuclei, it should be possible to obtain the fusion probability by considering the survival probability of the CN produced (through the total ER cross section). In this manner, the effect of the $N=126$ neutron shell on the production of Th isotopes in $^{40}Ar+Hf$ reactions has been widely discussed [11,12]. The apparent absence of shell effects (no increase in the production of Th isotopes with $N\simeq 126$) was explained in terms of an enhanced level density in the fission channel, giving rise to a strong competition with the particle-evaporation channels that lead to spherical nuclei [11]. However, bearing in mind the results of Ref. [10] and the latest work [13], these low production cross sections could also result from the reduced fusion probabilities [8–10]. In other words, the influence of QF on the production of ERs (through a reduction of CN formation) might be incorrectly assigned to the shell structures in the decaying nuclei.

In this work, we present measurements and analysis of the ER and fission excitation functions obtained in very asymmetric $^{12}C+^{204,206,208}Pb$ reactions leading to $^{216,218,220}Ra^*$, and in the more symmetric $^{48}Ca+^{168,170}Er$ reactions leading to $^{216,218}Ra^*$. The role of QF in the C+Pb reactions appears to be negligible, and so its excitation functions are a good reference point for applying the potential-barrier-passing

*Email address: sagaidak@sunvas.jinr.ru

(PBP) model for fusion and the standard statistical model (SSM) for describing the deexcitation of the CN [14]. Excitation functions for the production of Ra isotopes in the C + Pb reactions cover the region of neutron numbers $122 \leqslant N \leqslant 130$, so the $N=126$ shell could, in principle, manifest itself here. The results of the C+Pb analysis will then be exploited in the study of ^{48}Ca+ ^{168,170}Er. In our recent work on ^{12}C+ ^{204}Pb and ^{48}Ca+ ^{168}Er [15], a prominent QF component was observed in the mass and energy distributions of fission fragments for the more symmetric system. Such studies should clarify the influence of QF on fusion in the asymmetric reactions, leading to superheavy nuclei [16].

The experiments were carried out using ion beams from the XTU Tandem + ALPI accelerator complex of the Laboratori Nazionali di Legnaro in the energy range $E_{\rm lab}=56$–90 MeV for ^{12}C (intensity 5–10 pnA) and $E_{\rm lab}=180$–208 MeV for ^{48}Ca (intensity 1–5 pnA). The targets were metal evaporations of highly enriched isotopes ^{204,206,208}Pb and ^{168,170}Er (150–200 μg/cm^2) onto thin carbon backings (15–20 μg/cm^2). The beam intensity was monitored continuously using four silicon surface-barrier detectors to measure Rutherford scattering from the target.

Fission fragments (quasifission plus CN fission) were detected by the two-arm time-of-flight (TOF) spectrometer CORSET [15,17,18] installed inside the scattering chamber. Each arm of the spectrometer consisted of a compact start detector and a stop x,y position-sensitive detector, both based on microchannel plates. The arms of the spectrometer were positioned so that the angle between the two detected fission fragments was $\vartheta_{\rm c.m.} \simeq 180°$. The data were analyzed event by event, the mass M and the total kinetic energy (TKE) of the fragments being deduced from the measured velocities and positions. Binary events with full momentum transfer were selected using folding correlations corresponding to the double-differential cross sections $\partial^2\sigma/\partial M \partial$ (TKE) [15,18]. These differential cross sections were used to deduce total fission cross sections integrated both in and out of the reaction plane. This angular integration was performed for the symmetric-mass component [15] with an angular distribution given by the statistical transition-state model [19] for both the ^{12}C and the ^{48}Ca induced reactions. The results are considered to give the CN-fission cross section.

Evaporation residues recoiling from the target were separated from the intense flux of beamlike particles using an electrostatic deflector (ED) [20]. The ED was set at $\vartheta_{\rm lab}=3°$ to the beam direction for the ^{12}C reactions and at $\vartheta_{\rm lab}=1°$ for the ^{48}Ca reactions in order to reduce the background of multiply scattered beam particles. For the ^{48}Ca reactions, the separated ERs passed through the start detector of the TOF system and were implanted into a silicon surface-barrier stop detector (SSBD) installed about 50 cm downstream. The resolution of this system allowed us to distinguish ERs unambiguously in the E-TOF spectra. For the ^{12}C reactions, the energy resolution ($\lesssim$30-keV full width at half maximum) of the SSBD for 5–10 MeV α-particles allowed us to identify various ^{216,218,220}Ra* evaporation channels from their known α energies and those of their daughter products. The ER cross sections obtained at 3° and 1° were integrated using a Gaussian fit to the measured angular distributions for ^{214}Ra produced in the ^{12}C+ ^{206}Pb reaction at $E_{\rm lab}=73$ MeV and for ERs detected in the ^{48}Ca+ ^{170}Er reaction at $E_{\rm lab}=204$ MeV. Angular distributions were measured by rotating the ED around the target position. The integrated cross sections were corrected for the ED transmission efficiency [20] using a Monte Carlo simulation developed for this purpose.

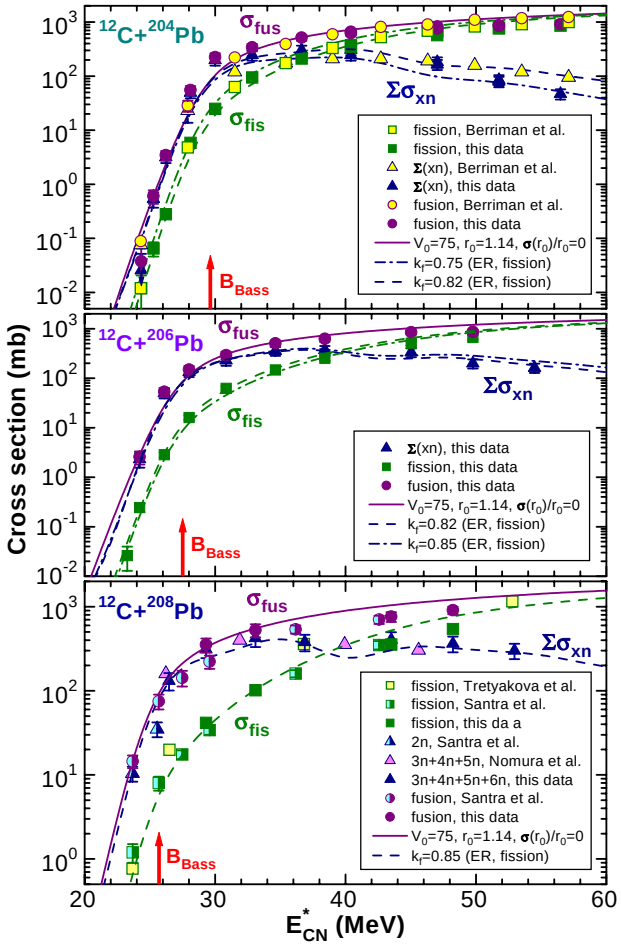

FIG. 1. (Color online) Measured excitation functions (symbols) for ERs (sum of the xn channels), fission, and fusion obtained in the ^{12}C+ ^{204,206,208}Pb reactions in comparison with the excitation functions calculated with HIVAP [14] (lines designated by $\Sigma\sigma_{\rm xn}$, $\sigma_{\rm fis}$, and $\sigma_{\rm fus}$), together with the values of the main parameters corresponding to the best fit to the data.

Figure 1 shows the excitation functions for ERs (sum of the xn channels), fission, and fusion (sum of the ER and fission cross sections) obtained for the ^{12}C+ ^{204,206,208}Pb reactions. The data obtained earlier in the ^{12}C+ ^{204,208}Pb reactions [10,21–23] are also shown. We observed no prominent α lines from residues corresponding to the light-charged-particle channels in the C+Pb reactions. This is consistent with our model predictions of smaller ER cross sections for light-charged-particle channels (pxn and αxn) and their significantly wider (or even different [24]) angular distributions. Figure 2 shows analogous quantities for the ^{48}Ca+ ^{168,170}Er reactions.

Our analysis of these data is performed in the framework of the PBP model and the SSM incorporated into the HIVAP

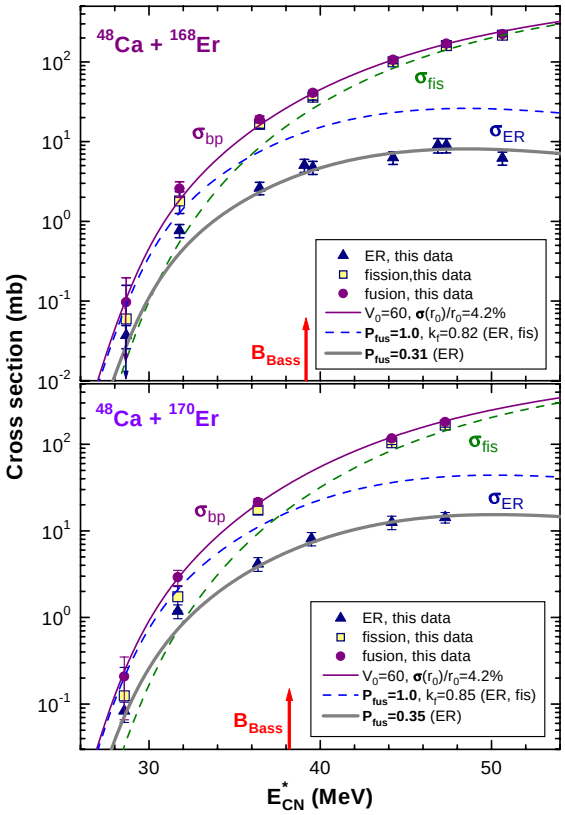

FIG. 2. (Color online) Measured excitation functions for ERs (sum of all evaporation channels), fission, and fusion obtained in the ^{48}Ca+^{168,170}Er reactions (symbols) in comparison with the excitation functions calculated with HIVAP [14] (lines designated by σ_{ER}, σ_{fis}, and σ_{bp}), together with the values of the main parameters corresponding to the best fit to the data and derived values of the fusion probability (P_{fus}).

code [14]. The calculated ER cross sections for strongly fissile CN at energies well above the fusion barrier [7] are relatively insensitive to the form of the nuclear potential [5,8], and are determined mainly by the SSM parameters describing the deexcitation of CN. The Reisdorf formula for the macroscopic parameters of the nuclear level density [14] leads to a ratio $\tilde{a}_f/\tilde{a}_\nu \gtrsim 1$ due to the different nuclear shapes at the saddle point (fission) and equilibrium state (particle emission). Ground-state shell effects were taken into account with a damping constant of 18.5 MeV [14,25], and were neglected at the saddle point. Empirical masses [26] were used to calculate the ground-state shell corrections [$\delta W_{g.s.}$ is the difference between the empirical and liquid-drop (LD) masses], as well as for excitation energies and separation energies. Our calculations at the energies above the fusion barrier depend only on one adjustable parameter k_f, i.e., the scaling factor of the rotating LD fission barriers, $B_f^{LD}(\ell)$ [27], is given by $B_f(\ell)=k_f B_f^{LD}(\ell)-\delta W_{g.s.}$.

Barrier-passing cross sections were calculated in the framework of the PBP model using the exponential nuclear potential with sharp radius corrections. The radius parameter r_0 was 1.14 fm for the C+Pb reactions and 1.12 fm for Ca +Er with a diffuseness $d=0.75$ fm in both cases. For the strength parameter of the nuclear potential, the best fit to the fusion data ($\sigma_{fus}=\sigma_{ER}+\sigma_{fis}$) yields $V_0=75$ MeV/fm for the C+Pb reaction and $V_0=60$ MeV/fm for Ca + Er. The values $r_0=1.14$ fm and $V_0=75$ MeV/fm were also found for the ^{16}O+^{208}Pb system (fusion of spherical nuclei) [28], whereas our analysis of the Ca+Er data gave us the same values ($r_0=1.12$ fm and $V_0=60$ MeV/fm) as those obtained for other systems involving deformed targets: ^{40}Ar+^{165}Ho $\cdots$ ^{181}Ta [12,29] and ^{40}Ar+^{148,154}Sm [30]. Barrier fluctuations, expressed through the radius-parameter ratio $\sigma(r_0)/r_0$, were generated with a Gaussian distribution of r_0 around its average value. The best fit to the C+Pb fusion cross sections corresponds to $\sigma(r_0)/r_0=0$, whereas for the Ca+Er data we obtained $\sigma(r_0)/r_0=4.2\%$. These r_0 fluctuations simulate couplings to the various entrance channels [30] to a degree sufficient for the present analysis. Transmission coefficients were obtained using the WKB approximation.

As we have seen in Fig. 1, a satisfactory fit to the ER and the fission excitation functions for the ^{12}C+^{204,206,208}Pb reactions allows us to extract k_f values. These values decrease from 0.85 to 0.75 as the neutron number decreases from 130 to 122, i.e., cross sections fall more rapidly than would follow from the calculations with a fixed value of k_f. The same tendency was found in the region from Rn to U with some additional reductions in the LD barriers around $N=126$ for Th, Pa, and U nuclei [9]. As already mentioned, the latter was assigned to a collective enhancement in the level density of the fission channel [11], which was effectively taken into account in the similar analysis [9] through the value of k_f. So, the manifestation of the $N=126$ shell, at least in the production of ^{214}Ra and its neighbors, is not distinctly observed in comparison with the production of more remote Ra nuclei.

The values of k_f obtained can be used in our analysis of the more symmetric ^{48}Ca+^{168,170}Er combinations. However, this leads to underestimates of fission cross sections at subbarrier energies and to marked overestimates of the ER cross sections at all energies (dashed lines in Fig. 2). This can be explained by the effect of QF inhibiting the fusion process, and we introduce fusion probabilities P_{fus} to reproduce the data. Their values, derived from the ratio of the calculated ER cross sections to the measured ones (thick gray lines in Fig. 2), are in the range 0.31–0.35. Performing the angle integration over all fission-fragment masses between the light and the heavy quasielastic peaks in the case of the ^{48}Ca reactions [15] [assuming a fission-fragment angular distribution $W(\overline{\vartheta}_{FF})\sim 1/\sin\overline{\vartheta}_{FF}$], one obtains an estimate of the total capture-fission cross sections (see, e.g., Ref. [31]). In this approach, considering the results as the total barrier-passing cross section, we obtain $V_0=70$ MeV/fm and, as a result of the higher total capture cross section, $P_{fus}=0.23$–0.30. These values are lower than those obtained for the more asymmetric ^{19}F+^{197}Au and ^{30}Si+^{186}W systems [10].

To be sure of the general character of our conclusion, we have applied our approach to the data of Ref. [10]. The results of the analysis are shown in Fig. 3. Neglecting some differences between the ^{12}C+^{204}Pb ER data obtained in our experiments and in Ref. [10] (which lead to opposite variations of k_f with excitation energy; from 0.75 to 0.82 accord-

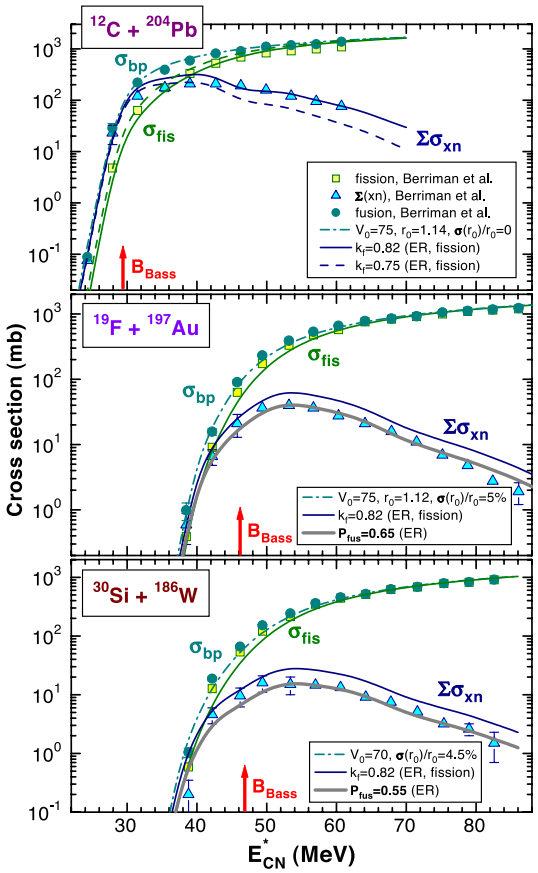

FIG. 3. (Color online) Same as in Figs. 1 and 2, but for the excitation functions (symbols) obtained in the ^{12}C+^{204}Pb, ^{19}F + ^{197}Au, and ^{30}Si+^{186}W reactions [10] and results of our analysis with HIVAP [14] (lines designated by $\Sigma\sigma_{xn}$, σ_{fis}, and σ_{bp}).

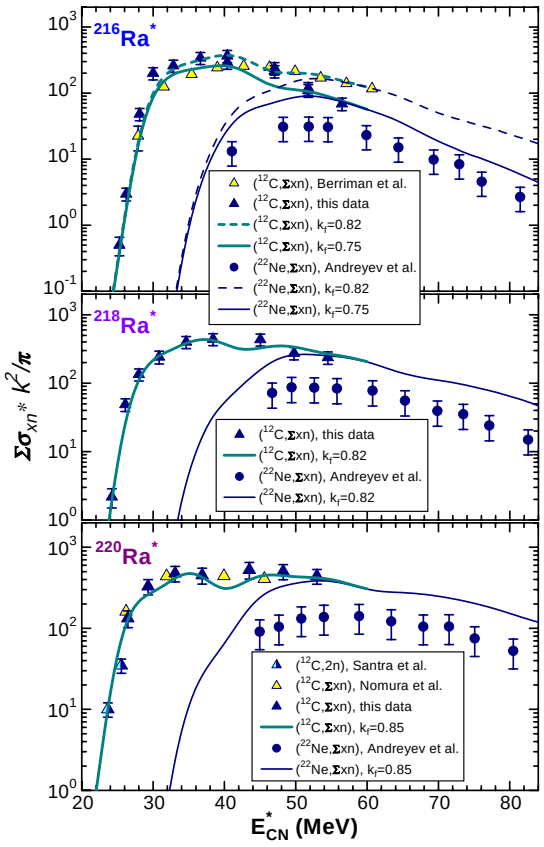

FIG. 4. (Color online) Reduced cross sections for the production of Ra nuclei in the ^{12}C+^{204,206,208}Pb and ^{22}Ne+^{194,196,198}Pt (systematic errors corresponding to 40% cross section values have been added to the data [32]) reactions (symbols) in comparison with results of our calculations with HIVAP [14] (lines).

ing to the data of Ref. [10] and from 0.82 to 0.75 according to our data at $E^*_{CN} \gtrsim 45$ MeV, see Figs. 2 and 3), we again obtain noticeable overestimates of the ER cross sections in the ^{19}F+^{197}Au and ^{30}Si+^{186}W reactions at energies well above the fusion barrier. The values of $P_{fus}=0.65\pm0.09$ and 0.55 ± 0.08 resulting from our analysis are similar to those (0.64 ± 0.09 and 0.57 ± 0.08) obtained for the ^{19}F and ^{30}Si induced reactions [10], confirming the consistency of our approach.

In Fig. 4, we compare the reduced ER cross sections (i.e., $\Sigma\sigma_{xn}k^2/\pi$, where k is the wave number) for the ^{12}C+^{204,206,208}Pb and ^{22}Ne+^{194,196,198}Pt [32] reactions (leading to the same ^{216,218,220}Ra* CN), as done earlier for more symmetric systems in Ref. [33] and recently in Refs. [10,13]. As we have seen, our calculations reproduce the C+Pb data and agree with similar calculations for Ne + Pt at energies well above the fusion barrier, where both reactions exhaust the angular momenta which may lead to evaporation. The experimental ER data do not converge, but show systematic differences between each pair of reactions, similar to the picture observed for the reactions leading to ^{216}Ra* [10] and ^{220}Th* [13], and confirming the important role of QF. Suppression factors for the ^{22}Ne induced reactions (P_{fus} in our notation) are estimated to be in the range 0.3–0.45.

The analysis presented in Figs. 1–3 implies that all partial waves passing through the potential barrier lead to fusion, i.e., $\sigma_{bp}=\sigma_{fus}\equiv\sigma_{CN}$ or $P_{fus}=1$ for the C+Pb systems. This is not the case for more symmetric massive systems. As shown in the radiochemical studies of reaction products from such systems [4,6] and in the analysis of ER production in asymmetric and nearly symmetric reactions leading to the same CN [8,9], σ_{fus} corresponds to a fraction of σ_{bp}, i.e., $P_{fus}<1$. Moreover, a similar situation is observed even for more asymmetric systems, as shown in Ref. [10] and also by the present data.

In conclusion, we have studied excitation functions for ERs and fission in ^{12}C+^{204,206,208}Pb reactions leading to ^{216,218,220}Ra*. Our analysis allowed us to fix the values of the main parameters describing the decay of the compound nuclei in the framework of the SSM [14]. By applying this model to the more symmetric ^{22}Ne+^{194,196,198}Pt and ^{48}Ca + ^{168,170}Er systems that lead to the same compound nuclei, we obtained noticeable overestimates of the ER cross sections at energies above and around the fusion barrier. We associate these overpredictions with a suppression of CN formation, corresponding to the fusion probabilities in the 0.23–0.45 range for both Ne + Pt and Ca+Er systems. These values are in qualitative agreement with the relative yield ($\simeq$30%) of the mass-asymmetric fission mode ob-

served in the $^{48}Ca+^{168}Er$ reaction [15]. This allows us to interpret this suppression, along with the mass-asymmetric fission mode in the ^{48}Ca reactions, as manifestations of the QF process. A more quantitative comparison of the ER and fission data can be performed only after measuring the angular distributions for both the mass-symmetric and mass-asymmetric fission modes. The suppression of ER production observed in the ^{22}Ne reactions is consistent with the unexpectedly high inhibition of fusion in the ^{19}F reaction [10].

The work was supported by the Russian Foundation for Basic Research (Grant Nos. 02-02-16116, 99-02-17891) and by INTAS (Grant No. 00-655).

[1] M. Dasgupta, D.J. Hinde, N. Rowley, and A.M. Stefanini, Annu. Rev. Nucl. Part. Sci. **48**, 401 (1998).
[2] J. Tōke *et al.*, Nucl. Phys. **A440**, 327 (1985).
[3] W.O. Shen *et al.*, Phys. Rev. C **36**, 115 (1987).
[4] W. Reisdorf *et al.*, Z. Phys. A **342**, 411 (1992).
[5] A.B. Quint *et al.*, Z. Phys. A **346**, 119 (1993).
[6] P. Klein *et al.*, Z. Phys. A **357**, 193 (1997).
[7] R. Bass, Lect. Notes Phys. **117**, 281 (1980).
[8] R.N. Sagaidak *et al.*, in *Proceedings of the International Conference on Shells-50, Dubna, 1999*, edited by Yu. Ts. Oganessian and R. Kalpakchieva (World Scientific, Singapore, 2000), p. 199.
[9] R.N. Sagaidak *et al.*, in *Proceedings of the International Workshop on Fusion Dynamics at the Extremes, Dubna, 2000*, edited by Yu. Ts. Oganessian and V.I. Zagrebayev (World Scientific, Singapore, 2001), p. 135.
[10] A.C. Berriman *et al.*, Nature (London) **413**, 144 (2001); D.J. Hinde *et al.*, J. Nucl. Radiochem. Sci. **3**, 31 (2002).
[11] A.V. Ignatyuk *et al.*, Yad. Fiz. **37**, 831 (1983) [Sov. J. Nucl. Phys. **37**, 495 (1983)].
[12] D. Vermeulen *et al.*, Z. Phys. A **318**, 157 (1984).
[13] D.J. Hinde, M. Dasgupta, and A. Mukherjee, Phys. Rev. Lett. **89**, 282701 (2002).
[14] W. Reisdorf, Z. Phys. A **300**, 227 (1981); W. Reisdorf and M. Schädel, *ibid.* **343**, 47 (1992).
[15] A.Yu. Chizhov *et al.*, Phys. Rev. C **67**, 011603(R) (2003).
[16] M.G. Itkis *et al.*, in *Proceedings of the International Workshop on Fusion Dynamics at the Extremes, Dubna, 2000*, edited by Yu. Ts. Oganessian and V.I. Zagrebayev (World Scientific, Singapore, 2001), p. 93.
[17] N.A. Kondratiev *et al.*, in *Proceedings of the fourth International Conference on Dynamical Aspects of Nuclear Fission, Častá-Papiernička, 1998*, edited by Yu. Ts. Oganessian *et al.* (World Scientific, Singapore, 1999), p. 431.
[18] I.V. Pokrovsky *et al.*, Phys. Rev. C **60**, 041304(R) (1999).
[19] R. Vandenbosch and J.R. Huizenga, *Nuclear Fission* (Academic, New York, 1973).
[20] S. Beghini *et al.*, Nucl. Instrum. Methods Phys. Res. A **239**, 585 (1985).
[21] T. Nomura *et al.*, Nucl. Phys. **A217**, 253 (1973).
[22] S.P. Tretyakova *et al.*, in *Proceedings of the International Conference on Shells-50, Dubna, 1999*, edited by Yu. Ts. Oganessian and R. Kalpakchieva (World Scientific, Singapore, 2000), p. 151.
[23] S. Santra *et al.*, Phys. Rev. C **64**, 024602 (2001).
[24] T. Nomura *et al.*, Phys. Rev. C **9**, 1168 (1974).
[25] A.V. Ignatyuk *et al.*, Yad. Fiz. **21**, 485 (1975) [Sov. J. Nucl. Phys. **21**, 255 (1975)].
[26] G. Audi and A.H. Wapstra, Nucl. Phys. **A595**, 509 (1995).
[27] S. Cohen *et al.*, Ann. Phys. (N.Y.) **82**, 557 (1974).
[28] C.R. Morton *et al.*, Phys. Rev. C **60**, 044608 (1999).
[29] H.-G. Clerc *et al.*, Nucl. Phys. **A419**, 571 (1984).
[30] W. Reisdorf *et al.*, Nucl. Phys. **A438**, 212 (1985).
[31] A.J. Pacheco *et al.*, Phys. Rev. C **45**, 2861 (1992).
[32] A.N. Andreyev *et al.*, Nucl. Phys. **A620**, 229 (1997).
[33] W. Reisdorf *et al.*, Nucl. Phys. **A444**, 154 (1985).